ZR | Zoological Research

Article   **Open Access**

Unexpected divergence in magnetoreceptor MagR from robin and pigeon linked to two sequence variations

Shun Wang[1,2], Peng Zhang[2,3], Fan Fei[2,3], Tianyang Tong[2,4], Xiujuan Zhou[2,3], Yajie Zhou[1,2], Jing Zhang[2,3], Mengke Wei[1,2], Yanqi Zhang[2,3], Lei Zhang[2,3], Yulong Huang[5], Lin Zhang[2], Xin Zhang[1,2,3,6], Tiantian Cai[2,3,*], Can Xie[2,3,6,*]

[1] *Institutes of Physical Science and Information Technology, Anhui University, Hefei, Anhui 230039, China*

[2] *High Magnetic Field Laboratory, Hefei Institutes of Physical Science, Chinese Academy of Sciences, Science Island, Hefei, Anhui 230031, China*

[3] *Science Island Branch of Graduate School, University of Science and Technology of China, Hefei, Anhui 230036, China*

[4] *Department of Anatomy, Anhui Medical University, Hefei, Anhui 230032, China*

[5] *Department of Mechanical and Aerospace Engineering, University at Buffalo, State University of New York, Buffalo, NY 14260 USA*

[6] *International Magnetobiology Frontier Research Center, Science Island, Hefei, Anhui 230031, China*

ABSTRACT

Birds exhibit extraordinary mobility and remarkable navigational skills, obtaining guidance cues from the Earth's magnetic field for orientation and long-distance movement. Bird species also show tremendous diversity in navigation strategies, with considerable differences even within the same taxa and among individuals from the same population. The highly conserved iron and iron-sulfur cluster binding magnetoreceptor (MagR) protein is suggested to enable animals, including birds, to detect the geomagnetic field and navigate accordingly. Notably, MagR is also implicated in other functions, such as electron transfer and biogenesis of iron-sulfur clusters, raising the question of whether variability exists in its biochemical and biophysical features among species, particularly birds. In the current study, we conducted a comparative analysis of MagR from two different bird species, including the migratory European robin (*Erithacus rubecula*) and the homing pigeon (*Columba livia*) . Sequence alignment revealed an extremely high degree of similarity between the MagRs of these species, with only three sequence variations. Nevertheless, two of these variations underpinned significant differences in metal binding capacity, oligomeric state, and magnetic properties. These findings offer compelling evidence for the marked differences in MagR between the two avian species, potentially explaining how a highly conserved protein can mediate such diverse functions.

Keywords: Homing and migration; Animal navigation; Magnetoreceptor (MagR); Diverse navigation pattern; Conserved protein

INTRODUCTION

Birds are among the most agile and mobile organisms in the animal kingdom, possessing an innate ability to navigate vast distances and reliably return to their points of origin. The Arctic tern (*Sterna paradisaea*) holds the record for the longest migration of any animal in the world, making a return trip of approximately 70 900 km from pole to pole each year (Egevang et al., 2010). Birds, as well as many other animals, can detect the Earth's magnetic field, which they utilize as a navigational tool to maintain spatial orientation and direction (Johnsen & Lohmann, 2008; Mouritsen, 2018; Wiltschko & Wiltschko, 2019). Homing and migration represent two distinct navigational strategies used by avian species, which are crucial for locating food sources and nesting sites (Dingle & Drake, 2007). The European robin (*Erithacus rubecula*), a widely distributed species across Europe, is noted for its semi-migratory behavior, with some populations moving between wintering grounds and summer breeding areas, and others remaining permanent residents throughout the year. In contrast, the pigeon (*Columba livia*) is one of the best-studied subjects for understanding animal homing behavior (Meade et al., 2005). The navigation systems of both the robin and pigeon have been extensively studied as model systems in the field of animal navigation.

For navigation, animals utilize two types of geomagnetic field cues: the vector of magnetic field lines, providing

directional information via polarity, and the gradient declines in magnetic intensity and inclination from the magnetic poles to the equator, which are integral components of the navigational "map" (Wiltschko & Wiltschko, 2019). In recent decades, several primary models have been proposed to explain how animals sense magnetic fields from different perspectives, including the magnetite-based model (Kirschvink et al., 2001), radical pair model (Hore & Mouritsen, 2016; Maeda et al., 2008; Rodgers & Hore, 2009; Xu et al., 2021), and biocompass model (Lohmann, 2016; Qin et al., 2016; Xie, 2022).

Magnetoreceptor (MagR), a highly conserved A‑type iron and iron‑sulfur cluster binding protein (Guo et al., 2021; Zhou et al., 2023) involved in the biogenesis of iron-sulfur clusters and electron transfer reactions (Bilder et al., 2004; Cózar-Castellano et al., 2004), has been suggested as a potential "universal mechanism for animal magnetoreception" in the biocompass model (Lohmann, 2016; Qin et al., 2016). However, the precise mechanism by which MagR may serve as a biocompass in response to the geomagnetic field is the subject of ongoing debate. Meister (2016) argued that the iron content in MagR is insufficient by several orders of magnitude to produce thermally induced fluctuations in the magnetic moment, while Nimpf & Keays (2022) suggested that the magnetic properties of MagR may result from laboratory contamination. Interestingly, several theories based on the MagR/Cry biocompass model, including long-range intermolecular electron transfer (Xie, 2022) and quantum mechanics (Cao & Yan, 2018; Xiao et al., 2020; Zhao et al., 2022), have provided alternative theoretical explanations of how MagR responds to the geomagnetic field. For example, Xiao et al. (2020) proposed a microscopic quantum dynamical model, which posits that radical pairs may facilitate geomagnetic field detection through induction of magnetic fluctuation in the MagR structure rather than permanent magnetism. Additionally, Arai et al. (2022) suggested that an external magnetic field may induce assembly of the MagR protein.

An increasing number of applications leveraging the magnetic properties of MagR have been reported, utilizing MagR or the MagR/Cry complex as magnetic tags (Jiang et al., 2017; Kang et al., 2021; Wang et al., 2019), bionic magnetic sensors (Cheng et al., 2023; Xue et al., 2020), and MRI contrast enhancers (Li et al., 2023). The functional significance of MagR has been extensively explored, with studies revealing daily oscillations in the expression patterns of MagR in certain species and higher expression levels in migratory populations, hinting at the physiological relevance of MagR in magnetoreception (Chang et al., 2017, 2018; Jin et al., 2023; Mannino et al., 2023). Notably, a recent *in vivo* study demonstrated that knockdown of MagR in oriental armyworms (*Mythimna separata*) abolished their magnetic orientation, suggesting a vital role of MagR in magnetoreception (Tong et al., 2022).

Considering the extensive variety of navigational strategies, such as homing and migration, across species, populations, and individuals in very different environments (Kentie et al., 2023), as well as the diverse functions attributed to MagR, the question arises: how does such a highly conserved protein function as a magnetoreceptor and mediate distinct biological processes? In our previous work, we determined that pigeon MagR (clMagR) binds to two types of iron-sulfur clusters, [2Fe-2S] and [3Fe-4S], each conferring distinct magnetic properties, suggesting a possible mechanism for magnetic modulation of MagR via iron-sulfur cluster binding (Guo et al., 2021). Additionally, we discovered that mononuclear iron and iron-sulfur clusters can both bind to pigeon MagR, with each element playing a synergistic and indispensable role in establishing the magnetic properties of clMagR (Zhou et al., 2023). Species-specific iron and iron-sulfur cluster binding has been confirmed in multiple species, from bacteria and yeast to pigeons and humans (Ding & Clark, 2004; Landry et al., 2013; Lill et al., 2012; Lu et al., 2010; Mühlenhoff et al., 2011; Ollagnier-De-Choudens et al., 2001; Yang et al., 2015; Zhou et al., 2023). Birds are the most species-rich class of tetrapod vertebrates and exhibit remarkable long-distance navigation abilities (Feng et al., 2020; Zhang et al., 2014). Therefore, it is important to investigate the diversity and conservation of magnetoreception in birds at the molecular level.

In the current study, MagRs from the migratory European robin and homing pigeon were analyzed and compared to investigate potential differences. Despite the high sequence identity (95.5%) between the robin MagR and pigeon MagR, unexpected biochemical and biophysical differences were identified. Notably, the robin MagR demonstrated much higher iron and iron-sulfur binding capacity and existed mainly as a dimer, where the pigeon MagR primarily presented as a tetramer. Only three variations in the sequences of robin MagR and pigeon MagR were found, with two contributing to the observed difference in metal binding and oligomerization. Our study clearly demonstrated the occurrence of marked and unexpected differences in two highly conserved avian MagR proteins, which may help explain the diverse functions and different but closely related navigational strategies (migration and homing) associated with such a conserved protein.

MATERIALS AND METHODS

Protein expression and purification
The expression vectors containing the pigeon and robin MagR genes were constructed with a Strep‑II tag on the N-terminal of MagR, as described previously (Qin et al., 2016; Zhou et al., 2023). The expression vectors of PtoR-K20R, PtoR-E47D, PtoR-delSAS, RtoP-R17K, RtoP-D44E, and RtoP-insSAS were obtained by site-directed mutagenesis (Tiangen, China) using robin MagR and pigeon MagR plasmid as templates in accordance with the manufacturer's instructions.

All proteins were expressed in the *Escherichia coli* strain BL21 (DE3). Bacterial cells were harvested after induction with 20 μmol/L isopropyl-D-1-thiogalactopyranoside (IPTG) at 288 K (15 °C) for 20–22 h. The cell culture was then harvested by centrifugation at 7 000 r/min for 8 min at 4 °C in 500 mL centrifuge bottles with a JA-10 rotor (Beckman Coulter, USA). To extract proteins, the cells were lysed by sonication on ice and resuspended in lysis buffer (20 mmol/L Tris, 500 mmol/L NaCl, pH 8.0). After centrifugation at 4 °C and 17 500 r/min for 45 min using a JA-20 rotor (Beckman Coulter, USA), the supernatant was collected and loaded onto a Strep-Tactin affinity column (IBA GmbH, Germany). The column was washed with approximately 20 column volumes (CV) of buffer W (20 mmol/L Tris, 500 mmol/L NaCl, pH 8.0) to remove unbound proteins. After washing, robin MagR, pigeon MagR protein, and their respective mutants were eluted from the Strep-Tactin affinity column with buffer E (20 mmol/L Tris, 150 mmol/L NaCl, 5 mmol/L d-desthiobiotin, pH 8.0). For sodium dodecyl-sulfate polyacrylamide gel electrophoresis

(SDS-PAGE), a protein ladder (PageRuler Prestained Protein Ladder, Thermo Scientific, Product# 26616, USA) was used as the molecular weight standard.

Ultraviolet-visible (UV-Vis) absorption analysis
Wild-type MagR and mutant proteins (100 µmol/L) were prepared in Buffer E (20 mmol/L Tris, 150 mmol/L NaCl, 5 mmol/L d-desthiobiotin, pH 8.0). UV-Vis spectra were recorded using a NanoDrop spectrophotometer (NanoDrop OneC, Thermo Scientific, USA) at room temperature in the near UV-Vis range (300–600 nm). Buffer E was used as the blank control.

Size‐exclusion chromatography (SEC)
Analytical SEC was used to monitor and distinguish various oligomeric states of MagR and its mutants. Purified proteins were injected into a Superdex 200 10/300 column (GE Healthcare, USA) connected to a GE AKTA FPLC purifier system at a flow rate of 0.50 mL/min. Columns were pre-equilibrated with TBS buffer (20 mmol/L Tris, 150 mmol/L NaCl, pH 8.0).

Cross-linking assay
Purified robin MagR and pigeon MagR were prepared in 10 mmol/L PBS at 100 µmol/L, then incubated with 1 mmol/L cross-linking reagent BS3 (sulfo-DSS, bis (sulfosuccinimidyl) suberate, Thermo Fisher Scientific, USA) at room temperature for 10 min. The reaction was then quenched with 100 mmol/L Tris-HCl (pH 8.0) for 15 min.

Ferrozine assay
Ferrous iron reacts with ferrozine to form an intense, purple-colored complex that can be quantified spectrophotometrically at 562 nm using a microplate reader. A series of ferric chloride (0–800 µmol/L) in 1 mol/L HCl was used to generate a standard curve. Total iron content in the MagRs and their mutant proteins was quantified by reducing iron with hydroxylamine hydrochloride (HAHCl, 10% (w/v) HAHCl in 1 mol/L HCl) and performing analysis using the ferrozine assay based on the stand curve, as described previously (Zhou et al., 2023). In brief, the protein and HAHCl mixtures (80 µL of HAHCl and 20 µL of proteins at 100 µmol/L, total 100 µL) were incubated at 37 °C for 30 min in the dark in a 96-well plate, followed by the addition of 100 µL of ferrozine reagent (0.1% (w/v) ferrozine in 50% (w/v) ammonium acetate) in each well and incubation at 37 °C for an additional 15 min in the dark. The iron-ferrozine complex was measured at 562 nm on a microplate reader (Tecan Spark, Switzerland). Total iron content in the MagRs and mutants was calculated based on the standard curve by linear regression analysis. There were three replicates for each protein sample. Histograms and statistical analyses were performed using GraphPad Prism v8.0. Student's t-test was used to test for differences in total iron between protein samples, with significance determined at $P<0.05$.

Circular dichroism (CD) spectroscopy
CD spectroscopy is a robust method for evaluating secondary structures in proteins in the far UV range (190–260 nm) or for monitoring protein-bound co-factors such as metals or iron-sulfur clusters in the near UV-vis range (300–600 nm) (Kelly & Price, 2000). To characterize protein-bound metals and iron-sulfur clusters, purified robin MagR and pigeon MagR (100 µmol/L) were measured using a CD MOS-500 spectrometer (Biologic, France) at room temperature with 1 cm path quartz

cells. Phosphate-buffered saline (PBS) buffer (0.01 mol/L, NaCl, $Na_2HPO_4·12H_2O$, $NaH_2PO_4·2H_2O$, pH 7.4) was used as a blank control.

Electron paramagnetic resonance (EPR) measurement
X-band (9.6 GHz) EPR spectra of the MagR proteins were recorded using an EMX plus 10/12 spectrometer (Bruker, USA), equipped with an Oxford ESR-910 liquid helium cryostat. Briefly, 1 mmol/L oxidized proteins (as-purified) in buffer E (20 mmol/L Tris, 150 mmol/L NaCl, 5 mmol/L d-desthiobiotin, pH8.0) were mixed in a total volume of 200 µL with 50 µL of glycerol, respectively. The 1 mmol/L reduced proteins were obtained by adding 2 µL of $Na_2S_2O_4$ (1 mol/L) to the protein samples. The protein samples were then transferred into a 4 mm diameter quartz EPR tube (Wilmad 707-SQ-250 M, USA) and frozen in liquid nitrogen. The EPR signals of the oxidized and reduced proteins were recorded at different temperatures (10, 25, 45, and 60 K). The EPR conditions were: microwave frequency, 9.4 GHz; microwave power, 2 mW; modulation frequency, 100 kHz; modulation amplitude, 2 G; receive gain, $1.0×10^4$.

Magnetic measurement
Protein samples, including wild-type robin MagR and pigeon MagR (in buffer E containing 20 mmol/L Tris, 150 mmol/L NaCl, 5 mmol/L D-desthiobiotin, pH 8.0) and blank control (buffer E), were lyophilized using a freezer dryer (Heto PowerDry LL3000, Thermo Scientific, USA). Magnetic measurements were performed on lyophilized samples (mass of approximately 5 mg) using a MPMS-3 magnetometer (Quantum Design, USA) equipped with a superconducting quantum interference device (SQUID) sensor at different temperatures (300 and 5 K). The fields applied were between −2 and 2 T. MH curves (magnetization (M) curves measured versus applied fields (H)) of proteins were obtained after subtracting the background from the buffer control. The volume magnetic susceptibility versus magnetic field of robin and pigeon MagRs were calculated based on the collected data, with a protein density of about 0.15 g/cm^3 (Beech et al., 2015).

RESULTS

Divergent features of robin and pigeon MagRs with highly conserved sequences
Although various navigational behaviors have been observed in animals, the underlying mechanisms remain unclear. MagR has been suggested to play an essential role in animal magnetoreception. The MagR sequence is highly conserved across species (Supplementary Figure S1), especially in birds (Figure 1A). However, the degree to which MagRs from different avian species with closely related sequences share functional characteristics is not yet known. In this study, we examined MagRs from the migratory European robin and non-migratory homing pigeon to explore their species-specific traits. The MagR sequences from the two species displayed a high degree of conservation, sharing 95.5% identity, with variations in only three regions (Figure 1A).

To determine whether the three variable regions or less conserved sites influence MagR functionality, we conducted comparative analysis of co-factor binding and oligomeric states of MagR proteins from different avian species, using the prokaryotic homologous protein IscA from *E. coli* as the control in some experiments. Strep-tagged MagRs from robin
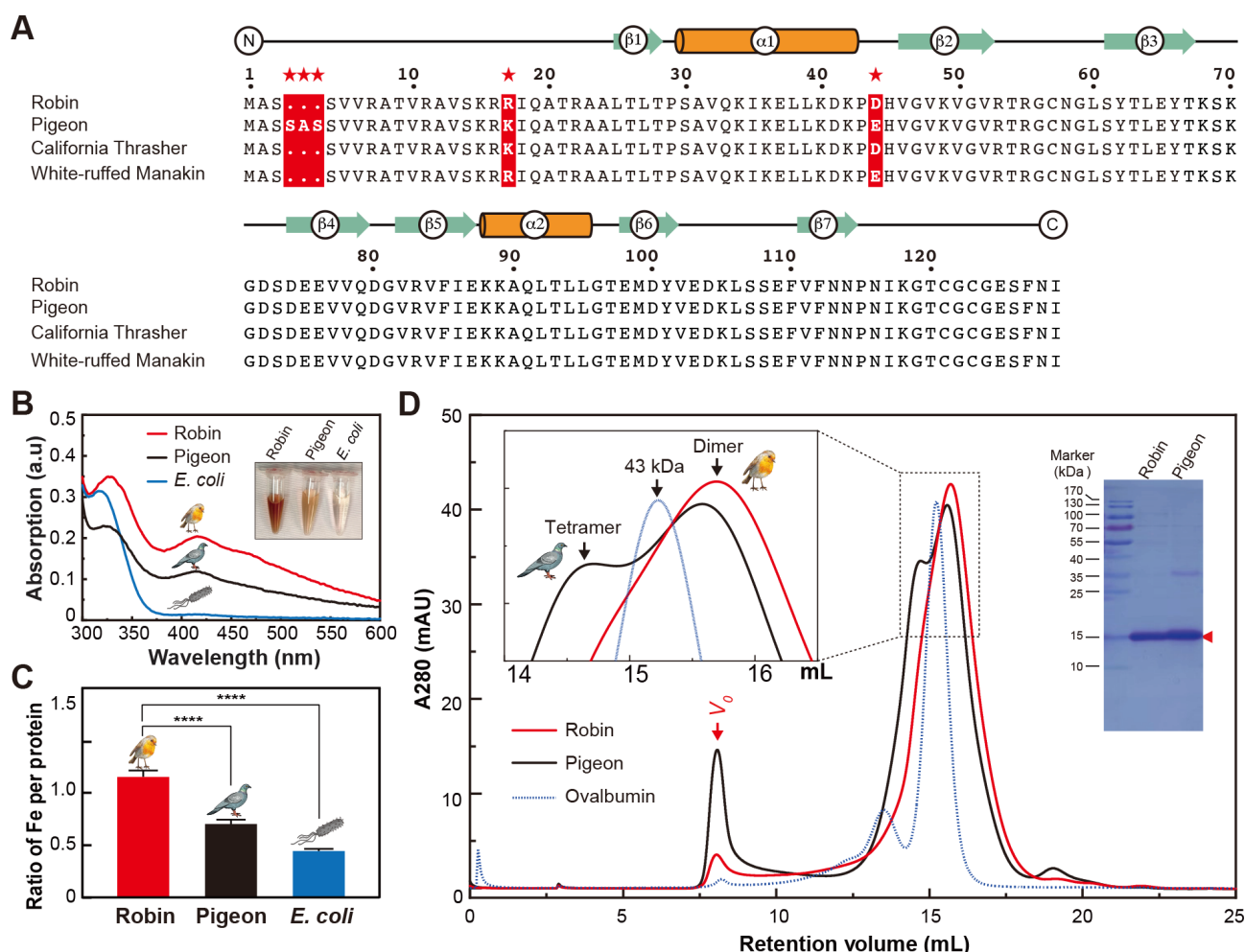
Figure 1 Differences in highly conserved avian MagRs

A: Sequence alignment of MagR from four different species of birds. Predicted secondary structures are shown in upper lines. Sequence variation sites are shown in white with a red background and marked by red stars (see Methods and Supplementary Materials for details about sequence ID). B: UV-Vis absorption spectra of robin MagR (red line), pigeon MagR (black line), and *E. coli* IscA (blue line). Insert pictures show color variation of MagR proteins in solution at a concentration of 800 µmol/L. C: Total iron content in purified robin MagR, pigeon MagR, and *E. coli* IscA measured by ferrozine assay as the ratio of iron atoms per protein monomer. Student's *t*-test, ****: $P<0.0001$, error bars represent mean±standard error of the mean (*SEM*). D: SEC of robin MagR (red line) and pigeon MagR (black line) analyzed using a Superdex 200 10/300 GL column. Ovalbumin (blue, dashed line) was used as a control to reveal elution volume of globular protein with relative molecular mass around 43 kDa. Arrows indicate voids (red) and peaks corresponding to MagR dimer and tetramer (black). SDS-PAGE of protein preparation under reducing conditions is shown as insert.

and pigeon and *E. coli* IscA were expressed and purified under aerobic conditions. UV-Vis absorbance spectra from 300 nm to 600 nm were measured to characterize iron and iron-sulfur cluster binding in MagR proteins. Significant differences in the UV-Vis profile were observed (Figure 1B). The robin and pigeon MagRs showed typical absorption peaks at 320 and 420 nm and a shoulder at 456 nm, indicating the presence of iron-sulfur cluster binding in the protein, consistent with previous reports (Guo et al., 2021; Zhou et al., 2023). In contrast, *E. coli* IscA only showed an absorption peak at 320 nm, suggesting iron binding but the absence of iron-sulfur clusters (Ding & Clark, 2004). Interestingly, robin MagR showed markedly higher UV-Vis absorption than pigeon MagR and *E. coli* IscA, in accordance with the coloration of protein solutions (as shown in Figure 1B). Freshly purified robin MagR was deep brown, pigeon MagR was light brown, and *E. coli* IscA was colorless at the same concentration. Total iron content was highest in robin MagR, followed by pigeon MagR and *E. coli* IscA, as quantified by ferrozine assay (Figure 1C).

There were notable differences in the oligomerization of MagR between the two avian species. Analytical SEC revealed that robin MagR exhibited a major peak with a retention volume of 16.0 mL, while pigeon MagR exhibited two major peaks with retention volumes of 15.02 and 15.89 mL, respectively. Comparing with ovalbumin, a reference protein with a 43 kDa mass that elutes at 15.54 mL, robin MagR was predominantly found in dimer form, whereas pigeon MagR exhibited a combination of dimers and tetramers in solution (Figure 1D), in alignment with the molecular weights of the robin and pigeon MagR monomers (16.18 and 16.41 kDa, respectively) determined by reducing SDS-PAGE. The formation of MagR dimers and tetramers was further confirmed by chemical crosslinking assay (Supplementary Figure S2).

Collectively, despite minimal sequence variations, robin MagR demonstrated a significantly greater capacity for binding iron and iron-sulfur compared to pigeon MagR and was consistently found as a dimer in solution, unlike the mixture of dimers and tetramers observed with pigeon MagR.

Pigeon MagR showed more stable iron-sulfur cluster binding compared to robin MagR

To elucidate the types and stabilities of iron-sulfur clusters in MagR across different species, the robin and pigeon MagR proteins were assessed using EPR, CD (300–600 nm), and UV-Vis absorption spectroscopy. The EPR spectra revealed identical g values for both the oxidized and reduced states of robin MagR and pigeon MagR (Supplementary Figure S3A–D), consistent with previous research (Guo et al., 2021). Correspondingly, the CD spectra of robin and pigeon MagRs showed similar signal profiles, including two positive peaks at 371 and 426 nm and three negative peaks at 324, 396, and 463 nm (Supplementary Figure S3E), indicating the presence of [2Fe-2S] and [3Fe-4S] clusters.

However, unexpected differences in the stability of iron-sulfur clusters between robin and pigeon MagRs were also observed. Freshly purified MagR proteins (200 μmol/L) were incubated at room temperature for 168 h and monitored by UV-Vis scanning every couple of hours. A reduction in the iron-sulfur cluster content in the MagR proteins was revealed by the decrease in absorption in UV-Vis spectra. As depicted in Figure 2A, B, robin MagR exhibited much higher UV-Vis absorption compared to pigeon MagR initially, indicating greater iron-sulfur cluster binding in robin MagR compared to pigeon MagR (as also seen in Figure 1A, C). During incubation, the UV-Vis absorption of both MagR proteins decreased with time, eventually reaching similar absorption

levels after 168 h, reflecting the dissociation or decay of the iron-sulfur clusters. The decrease in UV-Vis absorption at 320 and 420 nm was much faster for robin MagR than for pigeon MagR, suggesting a lower stability of iron-sulfur clusters in the former, despite its higher initial cluster binding (Figure 2C, D).

Differences in robin and pigeon MagRs can be traced to two sequence variations

Marked divergence in the properties of an identical protein from two closely related species with high sequence identity is atypical. To determine the key sequence variations responsible for the differences in MagR proteins, we generated a series of substitution mutants based on robin and pigeon MagR sequence alignment to convert robin MagR to pigeon MagR (abbreviated as "RtoP", Figure 3A) and *vice versa* (abbreviated as "PtoR", Figure 4A).

The wild-type and mutant MagRs (three RtoP mutants and three PtoR mutants) were then expressed and purified to homogeneity under aerobic conditions. UV-Vis spectral analysis showed that all mutants exhibited typical absorption at 320 and 420 nm, and a shoulder at 456 nm, indicating that the mutations did not change the iron-sulfur cluster binding type in the MagR proteins (Figures 3B, 4B), as confirmed by CD spectral analysis (Figures 3E, 4E).

Two of the three "RtoP" single-site substitutions or insertions, specifically RtoP-R17K (R17 to lysine substitution) and RtoP-insSAS (SAS insertion), showed a significant decrease in UV-Vis absorption, resembling that of pigeon
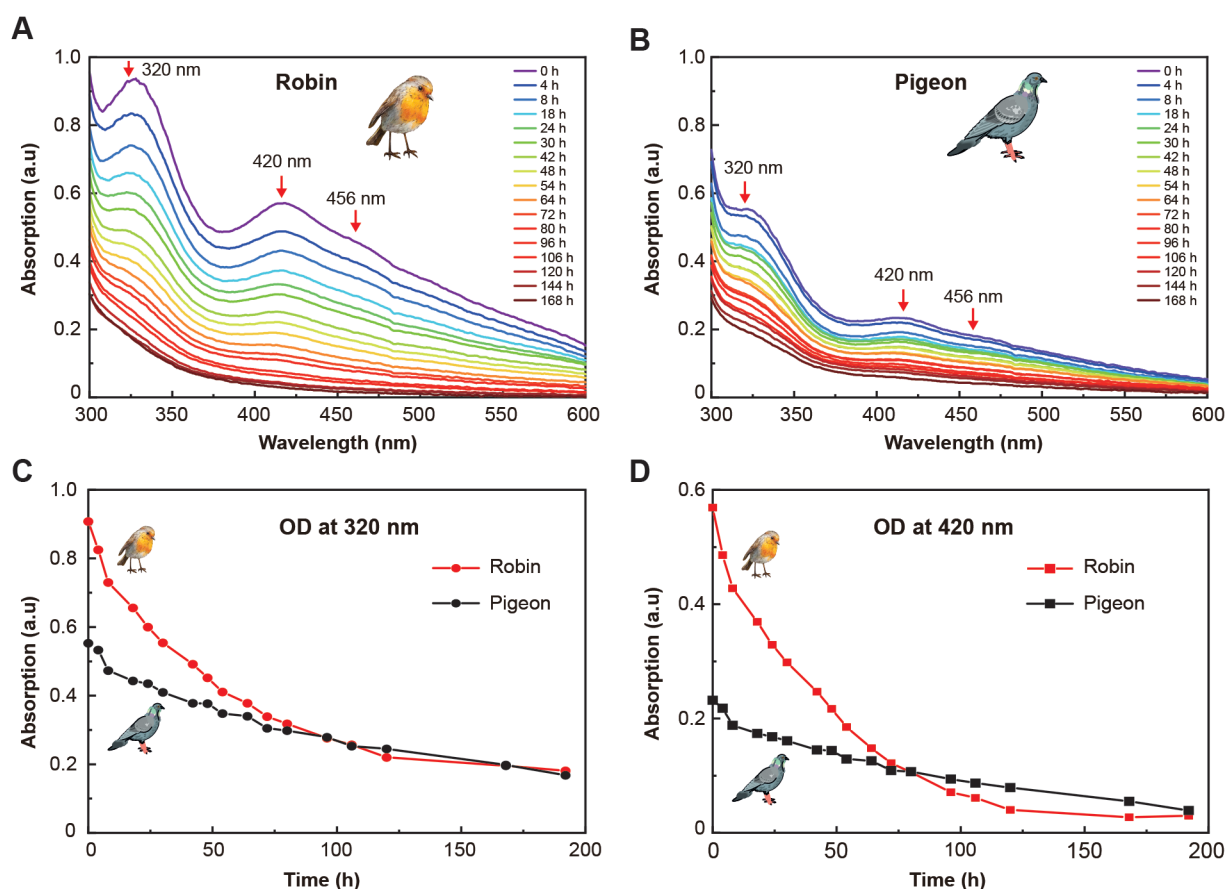

Figure 2 Stability of iron-sulfur cluster binding in robin MagR and pigeon MagR
A, B: UV-Vis absorption of purified robin MagR (A) and pigeon MagR (B) recorded at room temperature for 168 h. C, D: Decay curve of UV-Vis absorption of purified robin MagR and pigeon MagR at 320 nm (C, filled circles) and 420 nm (D, filled squares) during room temperature incubation. Data were derived from A and B.
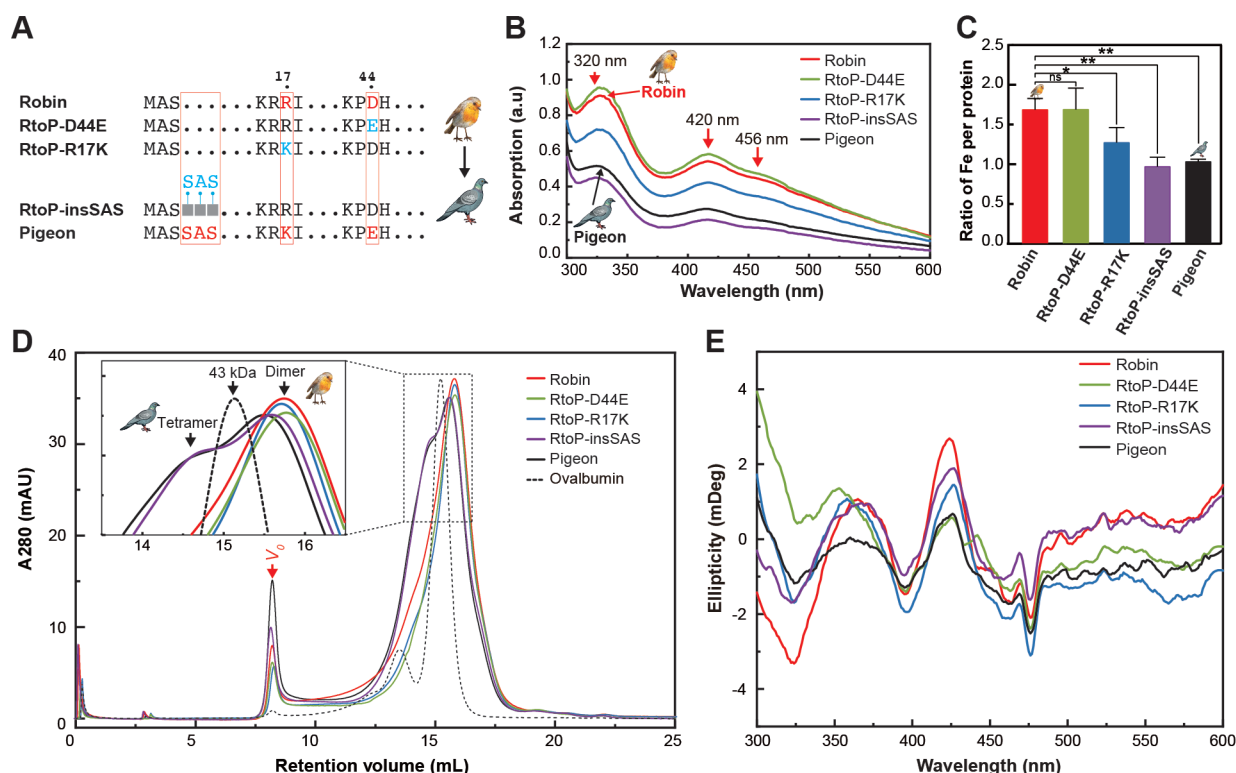
Figure 3 Differences in robin MagR and pigeon MagR are determined by two sequence variations, validated by "robin to pigeon" (RtoP) mutations

A: Robin to pigeon (RtoP) mutation design based on sequence alignment of robin MagR and pigeon MagR. Mutated amino acids are shown in blue. B: UV-Vis absorption of purified robin MagR (red line), its mutants (RtoP-D44E (green line), RtoP-R17K (blue line), and RtoP-insSAS (purple line)), and pigeon MagR (black line). C: Total iron content in purified robin MagR, its mutants (RtoP-D44E, RtoP-R17K, RtoP-insSAS), pigeon MagR, as measured by ferrozine assay. Student's t-test, [*]: $P<0.05$; [**]: $P<0.005$; ns: $P>0.05$, no significance. Error bars represent mean±*SEM*. D: SEC of wild-type robin MagR (red line), RtoP-D44E (green line), RtoP-R17K (blue line), RtoP-insSAS (purple line), pigeon MagR (black line), and ovalbumin (black, dashed line) analyzed on Superdex 200 10/300 GL column. Arrows indicate void (red) and two major peaks representing dimeric MagR and tetrameric MagR (black). E: CD spectra of as-purified robin MagR (red line), its mutants (RtoP-D44E (green line), RtoP-R17K (blue line), RtoP-insSAS (purple line)), and pigeon MagR (black line) measured at a concentration of 100 μmol/L.

MagR, while RtoP-D44E (D44 to glutamic acid) remained unchanged, displaying almost the same absorption as robin MagR (Figure 3B). Consistently, total iron content in RtoP-R17K and RtoP-insSAS decreased significantly compared to robin MagR but was approximately equivalent to pigeon MagR, whereas RtoP-D44E remained unchanged, akin to robin MagR (Figure 3C). Similar trends were observed in the oligomerization of the two wild-type MagRs and three RtoP mutants (Figure 3D), especially the "RtoP" mutant RtoP-insSAS (purple line in Figure 3D), which showed an almost identical oligomeric state as pigeon MagR. Thus, these findings suggested the N-terminal sequence insertion SAS and R17 in robin MagR (corresponding to K20 in pigeon) may play an active role in iron and iron-sulfur binding, and the SAS site may also contribute to tetramer formation and the modulation of higher order assembly in MagR.

Similarly, mutations were engineered to convert pigeon MagR to robin MagR (herein named "PtoR") to verify which sequence variations account for the observed differences (Figure 4A). Mutants PtoR-delSAS (deletion of N-terminal sequence SAS from pigeon sequence) and PtoR-K20R (substitution of K20 in pigeon sequence to R as in robin sequence) both exhibited significantly increased UV-Vis absorption (Figure 4B) and higher iron content (Figure 4C) compared to the wild-type pigeon MagR, closely resembling the pattern observed in robin MagR. Deletion of the N-terminal

SAS sequence from pigeon MagR successfully converted the oligomeric state to a dimeric state, almost identical to that of robin MagR (Figure 4D). These results suggest that the N-terminal sequence SAS and K20 in pigeon (corresponding to R17 in robin) may play active roles in iron and iron-sulfur binding, and the SAS site may also be involved in tetramer formation and the modulation of higher order assembly in MagR.

Robin MagR and pigeon MagR show different magnetic properties

As described above, robin MagR contained higher iron and iron-sulfur content than pigeon MagR. To explore whether differences in iron and iron-sulfur content influence magnetic properties of MagR, the magnetic moments of robin MagR and pigeon MagR were measured using SQUID (MPMS3) magnetometry at varying temperatures (300 and 5 K). MH curves were then generated to compare the magnetic susceptibility of both proteins (Figure 5A, B). The MH curves of both MagRs exhibited similar diamagnetic properties at 300 K and paramagnetic properties at 5 K, although robin MagR demonstrated slightly stronger paramagnetic effects than pigeon MagR. Overall, the magnetic susceptibility of robin MagR was approximately 2.6 times that of pigeon MagR.

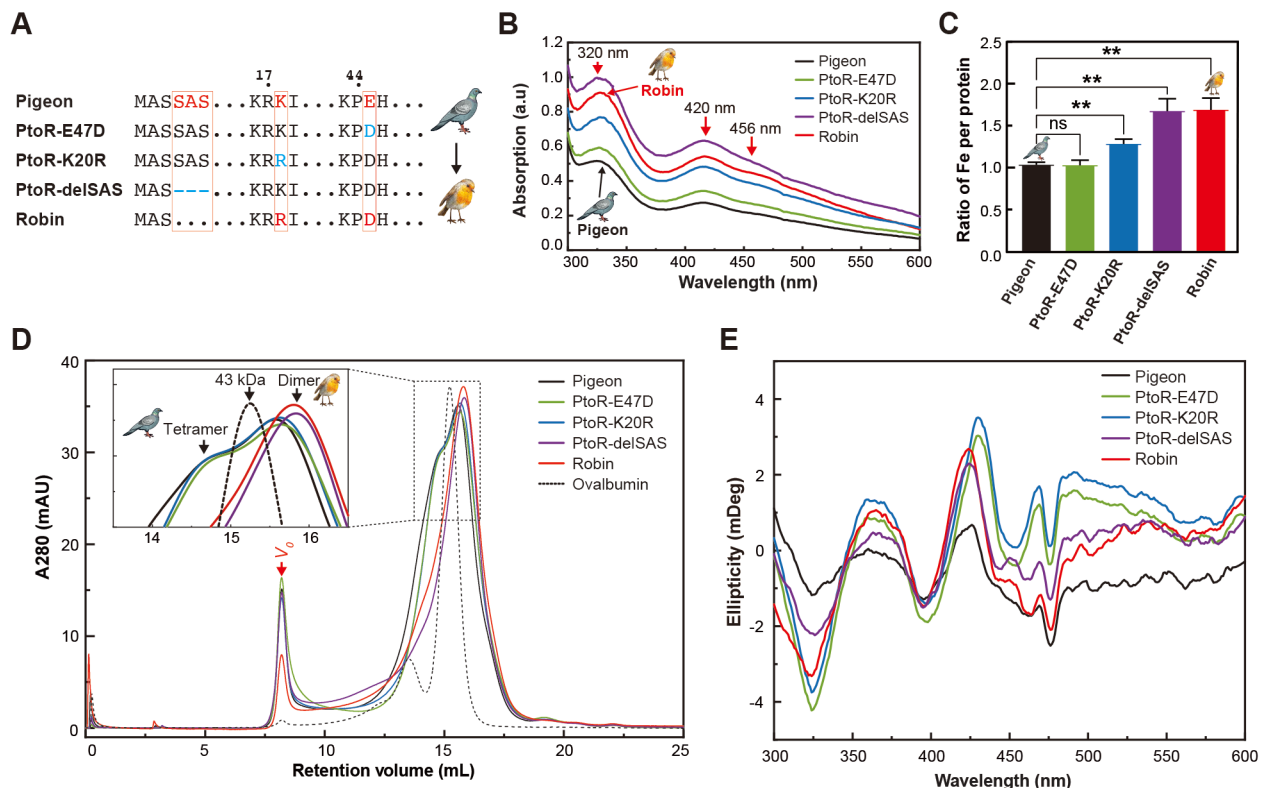To compare the magnetic susceptibilities of MagR to the known volume magnetic susceptibilities of typical tissues

Figure 4 Differences in robin MagR and pigeon MagR are determined by two sequence variations, as validated by "pigeon to robin" (PtoR) mutations

A: Pigeon to robin (PtoR) mutation design based on sequence alignment of pigeon and robin MagR. Mutated amino acids are shown in blue. B: UV-Vis absorption of purified pigeon MagR (black line), its mutants (PtoR-E47D (green line), PtoR-K20R (blue line), and PtoR-delSAS (purple line)), and robin MagR (red line). C: Total iron content in purified pigeon MagR, its mutants (PtoR-E47D, PtoR-K20R, and PtoR-delSAS), and robin MagR, as measured by ferrozine assay. Student's *t*-test, **: $P<0.005$; ns: $P>0.05$, no significance. Error bars represent mean±*SEM*. D: SEC of pigeon MagR (black line), PtoR-E47D (green line), PtoR-K20R (blue line), PtoR-delSAS (purple line), robin MagR (red line), and ovalbumin (black, dashed line) analyzed on Superdex 200 10/300 GL column. Arrows indicate void (red) and two major peaks corresponding to tetrameric and dimeric MagR (black). E: CD spectra of as-purified pigeon MagR (black line), its mutants (PtoR-E47D (green line), PtoR-K20R (blue line), and PtoR-delSAS (purple line)), and robin MagR (red line) measured at a concentration of 100 µmol/L.

(Klohs & Hirt, 2021), we converted mass magnetic susceptibilities in CGS units of MagR to volume magnetic susceptibilities (Figure 5C, D). The volume magnetic susceptibilities of robin MagR and pigeon MagR were -1.4204×10^{-6} and -1.2808×10^{-6}, respectively, at 300 K, which are more paramagnetic than those of heart and brain tissues (-1.932×10^{-5} and -6.928×10^{-6}, respectively).

DISCUSSION

Navigation in animals, the innate ability of diverse species to find their way accurately without the aid of maps or tools, is an evolutionary adaptation to spatiotemporal fluctuations in resources (Dingle & Drake, 2007). However, when examining various species, there is a notable variation in navigational behaviors, even among members of the same taxonomic category. Various insect species may engage in annual migrations or multiple migrations within a breeding season across generations, while other species, such as honeybees and pigeons, adopt very different homing strategies. Additionally, some animals undertake round-trip migrations, whereas others embark on "one-way" migrations, often triggered by habitat deterioration or food scarcity.

Animal navigation usually manifests as either migration or homing, with both processes involving the movement of organisms within their environment. Migration typically refers to the regular, annual, or seasonal mass movements of animals that cycle between breeding grounds and wintering areas (Greenberg & Marra, 2005). In contrast, homing is the inherent ability of an animal (e.g., honeybees and pigeons) to return to a specific starting point from various locations, often navigating through unfamiliar territories over considerable distances. This considerable diversity in navigation patterns has led to speculation about whether a universal mechanism or magnetoreceptor is present in animals across different phyla.

MagR, along with its prokaryotic homologous protein IscA, is one of the most highly conserved and abundant proteins across all organisms, ranging from bacteria and yeasts to plants and animals. Upon its initial discovery and potential involvement in magnetoreception, one question was naturally raised: How might such a highly conserved protein contribute to the vast array of animal behaviors related to magnetoreception (including both migratory and residential species) and different navigation patterns? Therefore, in this study, we examined MagRs from two closely related avian species, the migratory robin and the homing pigeon, to elucidate the potential differences between their respective proteins.

The sequence identity between robin MagR and pigeon MagR reached 95.5% (with a similarity of 97%), with only
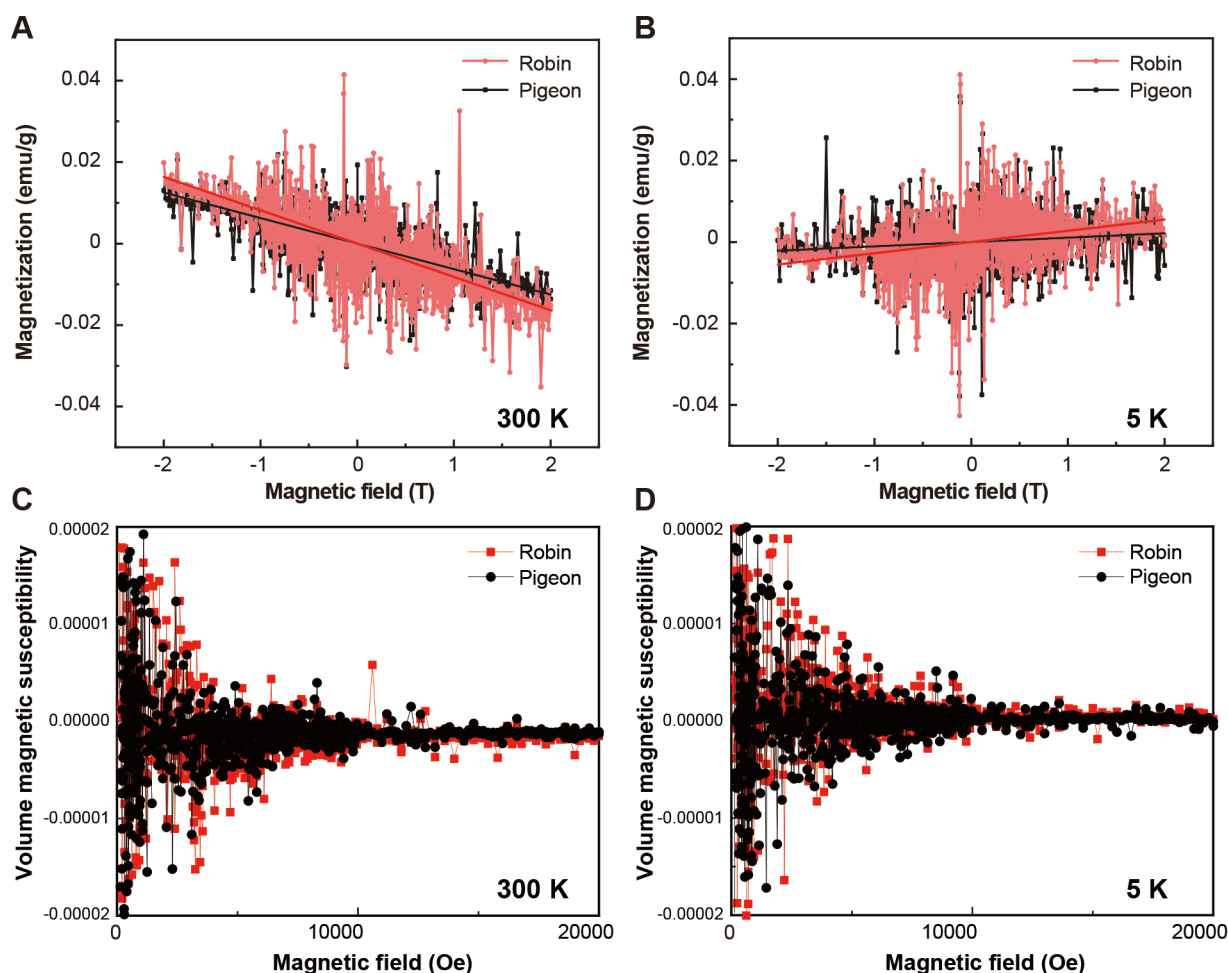
Figure 5 Robin MagR and pigeon MagR showed different magnetic properties
A: Field-dependent magnetization curves (MH) at 300 K for pigeon MagR (black) and robin MagR (red). Magnetic susceptibilities of pigeon MagR and robin MagR were –6.26395e-7 and –8.17783e-7, respectively. B: Field-dependent magnetization curves (MH) at 5 K for pigeon MagR (black) and robin MagR (red). Magnetic susceptibilities of pigeon MagR and robin MagR were 1.06894e-7 and 2.75509e-7, respectively. C, D: Volume magnetic susceptibility versus magnetic field of robin MagR (red) and pigeon MagR (black) at 300 K (C) and 5 K (D).

three sequence variations identified through alignment. Notable differences in the biochemical and biophysical properties of the two proteins were observed, including variations in iron and iron-sulfur binding capacities, oligomeric states, and magnetic features. These differences were attributed to the small sequence variations through site-directed mutagenesis, in which the robin-type was converted to the pigeon-type, and *vice versa*. The pronounced disparities in the MagR proteins between these two species prompted a reconsideration of the initial question: Can a protein with such conserved sequences be integral in both migratory and residential species, and potentially also be involved in diverse navigational behaviors? Based on the findings of this study, we propose that this is indeed plausible.

Proteins adapt through evolution to perform specific biological functions, with these functions shaping the divergence in their sequences. MagR follows this evolutionary pattern. Initially identified as a scaffolding protein for iron-sulfur cluster assembly and implicated in mitochondrial dysfunction syndrome in humans (Bilder et al., 2004; Cupp-Vickery et al., 2004; Jacobson et al., 1989; Ollagnier-De-Choudens et al., 2001), MagR was subsequently proposed as a putative magnetoreceptor upon the discovery of its interaction with cryptochrome (Cry). Both the redox potential

involved in electron transportation and magnetic properties relevant to animal magnetoreception may have influenced the evolutionary trajectory of MagR. Our findings indicated that the variable sequences or less conserved regions in the proteins evolved slowly, which may not directly impact primary protein function, but may exert significant influence on protein structure and stability. Consequently, these regions may contribute to the diversity of physiological functions across organisms, including animal magnetoreception and navigation patterns.

Several significant directions for future research are apparent. First, it is worth investigating whether the observed differences between MagRs from migratory species such as robins and homing species such as pigeons are reflective of their distinct migratory and homing behaviors. It is also possible that robin MagR and pigeon MagR may function similarly in magnetoreception and navigation, with the differing properties observed in this study being related to other MagR functions, such as iron-sulfur cluster biogenesis and electron transfer reactions. Therefore, the link between the biochemical properties of MagR and the diversity of navigational patterns remains an open question. Second, a comprehensive and comparative study of MagRs from a wide range of species across different phyla could be crucial in understanding the

biochemical and biophysical diversification of this ancient and highly conserved protein. Such research could illuminate the ways in which speciation and functional selection pressures for magnetoreception/navigation have driven sequence divergence and evolution of MagR, greatly enhancing our comprehension of the mechanisms underlying animal magnetoreception and navigation.

REFERENCES

Arai S, Shimizu R, Adachi M, et al. 2022. Magnetic field effects on the structure and molecular behavior of pigeon iron–sulfur protein. *Protein Science*, **31**(6): e4313.

Beech KE, Biddlecombe JG, Van Der Walle CF, et al. 2015. Insights into the influence of the cooling profile on the reconstitution times of amorphous lyophilized protein formulations. *European Journal of Pharmaceutics and Biopharmaceutics*, **96**: 247−254.

Bilder PW, Ding HG, Newcomer ME. 2004. Crystal structure of the ancient, Fe-S scaffold IscA reveals a novel protein fold. *Biochemistry*, **43**(1): 133−139.

Cao YS, Yan P. 2018. Role of atomic spin-mechanical coupling in the problem of a magnetic biocompass. *Physical Review E*, **97**(4): 042409.

Chang H, Fu XW, Zhao SY, et al. 2017. Molecular characterization, tissue, and developmental expression profiles of *MagR* and *Cryptochrome* genes in *Agrotis ipsilon* (Lepidoptera: Noctuidae). *Annals of the Entomological Society of America*, **110**(4): 422−432.

Chang H, Guo JL, Fu XW, et al. 2018. Molecular characterization and expression profiles of *IscA1* gene in a long-distance migrant. *Agrotis segetum. Journal of Asia-Pacific Entomology*, **21**(4): 1299−1306.

Cheng Q, Sun J, Ge Y, et al. 2023. Bionic magnetic sensor based on the MagR/Cry4 complex-configured graphene transistor with an integrated on-chip gate. *ACS Sens*, **8**(2): 793−802.

Cózar-Castellano I, Del Valle Machargo M, Trujillo E, et al. 2004. hIscA: a protein implicated in the biogenesis of iron-sulfur clusters. *Biochimica et Biophysica Acta (BBA) - Proteins and Proteomics*, **1700**(2): 179−188.

Cupp-Vickery JR, Silberg JJ, Ta DT, et al. 2004. Crystal structure of IscA, an iron-sulfur cluster assembly protein from *Escherichia coli. Journal of Molecular Biology*, **338**(1): 127–137.

Ding HE, Clark RJ. 2004. Characterization of iron binding in IscA, an ancient iron-sulphur cluster assembly protein. *Biochemical Journal*, **379**(2): 433−440.

Dingle H, Drake VA. 2007. What is migration?. *BioScience*, **57**(2): 113−121.

Egevang C, Stenhouse IJ, Phillips RA, et al. 2010. Tracking of Arctic terns *Sterna paradisaea* reveals longest animal migration. *Proceedings of the National Academy of Sciences of the United States of America*, **107**(5): 2078−2081.

Feng SH, Stiller J, Deng Y, et al. 2020. Dense sampling of bird diversity increases power of comparative genomics. *Nature*, **587**(7833): 252−257.

Greenberg R, Marra PP. 2005. Birds of Two Worlds: The Ecology and Evolution of Migration. Baltimore: Johns Hopkins University Press.

Guo Z, Xu S, Chen X, et al. 2021. Modulation of MagR magnetic properties via iron–sulfur cluster binding. *Scientific Reports*, **11**(1): 23941.

Hore PJ, Mouritsen H. 2016. The radical-pair mechanism of magnetoreception. *Annual Review of Biophysics*, **45**: 299−344.

Jacobson MR, Brigle KE, Bennett LT, et al. 1989. Physical and genetic map of the major *nif* gene cluster from *Azotobacter vinelandii. Journal of Bacteriology*, **171**(2): 1017–1027.

Jiang M, Zhang LJ, Wang FQ, et al. 2017. Novel application of magnetic protein: convenient one-step purification and immobilization of proteins. *Scientific Reports*, **7**(1): 13329.

Jin MH, Liu B, Zheng WG, et al. 2023. Chromosome-level genome of black cutworm provides novel insights into polyphagy and seasonal migration in insects. *BMC Biology*, **21**(1): 2.

Johnsen S, Lohmann KJ. 2008. Magnetoreception in animals. *Physics Today*, **61**(3): 29−35.

Kang J, Kang D, Yeom G, et al. 2021. Molecular diagnostic system using engineered fusion protein-conjugated magnetic nanoparticles. *Analytical Chemistry*, **93**(50): 16804−16812.

Kelly SM, Price NC. 2000. The use of circular dichroism in the investigation of protein structure and function. *Current Protein & Peptide Science*, **1**(4): 349−384.

Kentie R, Morgan Brown J, Camphuysen KCJ, et al. 2023. Distance doesn't matter: migration strategy in a seabird has no effect on survival or reproduction. *Proceedings of the Royal Society B:Biological Sciences*, **290**(1997): 20222408.

Kirschvink JL, Walker MM, Diebel CE. 2001. Magnetite-based magnetoreception. *Current Opinion in Neurobiology*, **11**(4): 462−467.

Klohs J, Hirt AM. 2021. Investigation of the magnetic susceptibility properties of fresh and fixed mouse heart, liver, skeletal muscle and brain tissue. *Physica Medica*, **88**: 37−44.

Landry AP, Cheng ZS, Ding HE. 2013. Iron binding activity is essential for the function of IscA in iron-sulfur cluster biogenesis. *Dalton Transactions*, **42**(9): 3100−3106.

Li N, Wang P, Xie YY, et al. 2023. Expression of clMagR/clCry4 protein in mBMSCs provides T_2-contrast enhancement of MRI. *Acta Biomaterialia*, doi:https://doi.org/10.1016/j.actbio.2023.09.039.

Lill R, Hoffmann B, Molik S, et al. 2012. The role of mitochondria in cellular iron-sulfur protein biogenesis and iron metabolism. *Biochimica et Biophysica Acta (BBA) - Molecular Cell Research*, **1823**(9): 1491−1508.

Lohmann KJ. 2016. A candidate magnetoreceptor. *Nature Materials*, **15**(2): 136−138.

Lu JX, Bitoun JP, Tan GQ, et al. 2010. Iron-binding activity of human iron-sulfur cluster assembly protein hIscA1. *Biochemical Journal*, **428**(1): 125−131.

Maeda K, Henbest KB, Cintolesi F, et al. 2008. Chemical compass model of avian magnetoreception. *Nature*, **453**(7193): 387−390.

Mannino G, Casacci LP, Bianco Dolino G, et al. 2023. The geomagnetic

field (GMF) is necessary for black garden ant (*Lasius niger* L.) foraging and modulates orientation potentially through aminergic regulation and *MagR* expression. *International Journal of Molecular Sciences*, **24**(5): 4387.

Meade J, Biro D, Guilford T. 2005. Homing pigeons develop local route stereotypy. *Proceedings of the Royal Society B:Biological Sciences*, **272**(1558): 17−23.

Meister M. 2016. Physical limits to magnetogenetics. *eLife*, **5**: e17210.

Mouritsen H. 2018. Long-distance navigation and magnetoreception in migratory animals. *Nature*, **558**(7708): 50−59.

Mühlenhoff U, Richter N, Pines O, et al. 2011. Specialized function of yeast Isa1 and Isa2 proteins in the maturation of mitochondrial [4Fe-4S] proteins. *Journal of Biological Chemistry*, **286**(48): 41205−41216.

Nimpf S, Keays DA. 2022. Myths in magnetosensation. *iScience*, **25**(6): 104454.

Ollagnier-De-Choudens S, Mattioli T, Takahashi Y, et al. 2001. Iron-sulfur cluster assembly: characterization of IscA and evidence for a specific and functional complex with ferredoxin. *Journal of Biological Chemistry*, **276**(25): 22604−22607.

Qin SY, Yin H, Yang CL, et al. 2016. A magnetic protein biocompass. *Nature Materials*, **15**(2): 217−226.

Rodgers CT, Hore PJ. 2009. Chemical magnetoreception in birds: the radical pair mechanism. *Proceedings of the National Academy of Sciences of the United States of America*, **106**(2): 353−360.

Tong DD, Zhang L, Wu NN, et al. 2022. The oriental armyworm genome yields insights into the long-distance migration of noctuid moths. *Cell Reports*, **41**(12): 111843.

Wang L, Xu HX, Liu ZW, et al. 2019. Magnetic immobilization of a quorum sensing signal hydrolase, AiiA. *Microbiologyopen*, **8**(8): e00797.

Wiltschko R, Wiltschko W. 2019. Magnetoreception in birds. *Journal of The Royal Society Interface*, **16**(158): 20190295.

Xiao DW, Hu WH, Cai YF, et al. 2020. Magnetic noise enabled biocompass. *Physical Review Letters*, **124**(12): 128101.

Xie C. 2022. Searching for unity in diversity of animal magnetoreception: from biology to quantum mechanics and back. *The Innovation*, **3**(3): 100229.

Xu JJ, Jarocha LE, Zollitsch T, et al. 2021. Magnetic sensitivity of cryptochrome 4 from a migratory songbird. *Nature*, **594**(7864): 535−540.

Xue L, Hu T, Guo Z, et al. 2020. A novel biomimetic magnetosensor based on magneto‐optically involved conformational variation of MagR/Cry4 complex. *Advanced Electronic Materials*, **6**(4): 1901168.

Yang J, Tan GQ, Zhang T, et al. 2015. Deletion of the proposed iron chaperones IscA/SufA results in accumulation of a red intermediate cysteine desulfurase IscS in *Escherichia coli*. *Journal of Biological Chemistry*, **290**(22): 14226–14234.

Zhang GJ, Li C, Li QY, et al. 2014. Comparative genomics reveals insights into avian genome evolution and adaptation. *Science*, **346**(6215): 1311−1320.

Zhao X, Chen HB, Lu LH, et al. 2022. A mechanism of compass-free migratory navigation. *Journal of Physics D:Applied Physics*, **55**(24): 245004.

Zhou YJ, Tong TY, Wei MK, et al. 2023. Towards magnetism in pigeon MagR: iron- and iron-sulfur binding work indispensably and synergistically. *Zoological Research*, **44**(1): 142−152.